metals

MDPI

Article

Biodegradable Behaviors of Ultrafine-Grained ZE41A Magnesium Alloy in DMEM Solution

Jinghua Jiang [1,2], Fan Zhang [1], Aibin Ma [1,*], Dan Song [1], Jianqing Chen [1], Huan Liu [1] and Mingshan Qiang [1]

Received: 10 October 2015; Accepted: 17 December 2015; Published: 23 December 2015
Academic Editors: Vineet V. Joshi and Alan Meier

[1] College of Mechanics and Materials, Hohai University, Nanjing 210098, China; jinghua-jiang@hhu.edu.cn (J.J.); zhangf416@gmail.com (F.Z.); songdancharls@hhu.edu.cn (D.S.); chenjq@hhu.edu.cn (J.C.); liuhuanseu@163.com (H.L.); 15751873896@163.com (M.Q.)
[2] Jiangsu Key Laboratory of Advanced Structural Materials and Application Technology, Nanjing 226000, China
* Correspondence: aibin-ma@hhu.edu.cn; Tel.: +86-25-8378-6046; Fax: +86-25-8378-7239

Abstract: The main limitation to the clinical application of magnesium alloys is their too-fast degradation rate in the physiological environment. Bio-corrosion behaviors of the ZE41A magnesium alloy processed by multi-pass equal channel angular pressing (ECAP) were investigated in Dulbecco's Modified Eagle Medium (DMEM) solution, in order to tailor the effect of grain ultrafining on the biodegradation rate of the alloy implant. Hydrogen evolution tests indicated that a large number of ECAP passes decreased the stable corrosion rate of the alloy after the initial incubation period. Potentiodynamic polarization curves showed that more ECAP passes made the corrosion potential nobler and the corrosion tendency lower. Corroded surfaces of the ECAPed alloy indicated a higher resistance toward localized corrosion due to the homogeneous redistribution of broken second phases on the ultrafine-grained Mg matrix. It suggests that grain ultrafining can decrease the biodegradable rate of the magnesium alloy-containing rare-earth elements and tailor the lifetime of the biodegradable material.

Keywords: magnesium alloy; biodegradation; ECAP; grain refinement; bio-corrosion

1. Introduction

Several million people suffer from bone fractures annually, which have to be surgically fixed by internal bone implants. Conventional inert metal implants (made of Ti alloys, stainless steels and Co-Cr alloys) have several disadvantages such as stress shielding and additional surgical intervention [1]. To overcome these drawbacks, biodegradable implants are of special interest for clinical applications. Most of the current biodegradable implants are made of polymers, which have relatively low strength and unpredictable degradation rates [2]. Therefore, magnesium and its alloys have garnered more and more attention for their excellent biocompatibility, elastic modulus and compressive yield strength, similar to those of human bone, and other positive effects on the growth of new bone after implanting in a physiological environment [3–5].

Magnesium alloys as biodegradation implants had already been applied to orthopedic and trauma surgery in the middle of the last century. However, the applications are seriously limited due to the excessively rapid degradation rate in the physiological environment [6,7]. Previous studies have shown that grain refinement can improve the corrosion resistance of some Mg alloys in Cl^--containing solution [8,9]. Equal-channel angular pressing (ECAP) is an effective technique to fabricate bulk ultrafine-grained (UFG) metallic materials with almost the same geometrical shape, and exceptional mechanical or/and physical advantages [8,10,11]. Until now, only a few studies have

been carried out to investigate the influence of ECAP on corrosion behaviors of magnesium and its alloys [12,13]. The limited literatures present that these ECAP procedures endow some magnesium alloys with higher corrosion resistance and better mechanical properties [8,9,14]. However, the corrosion results in NaCl solution cannot be used to perfectly predict biodegradation behaviors of magnesium alloys in the physiological environment. Therefore, particular attention should be paid to reveal the effect of ECAP on the bio-corrosion behavior of Mg alloys, in order to reveal the effect of grain ultrafining on the biodegradation rate of the alloy implant.

During the degradation of magnesium alloys, most alloying elements will dissolve into the human body. Therefore, the magnesium alloy containing Al, Cd and heavy metals is not appropriate for clinical application from the medical aspect [15]. The ZE41A magnesium alloy with low rare-earth (RE) content is suitable to act a biodegradable material since some RE elements are proven to be tolerated by the human body [14,16]. Our previous work showed that the ZE41A alloy after multi-pass ECAP consists of UFG Mg matrix and homogeneously dispersed second-phase particles, which contribute to better mechanical properties at room temperature and the higher corrosion resistance in NaCl solutions [17,18]. Thus, the aim of this paper is to study the biodegradation behavior of the ECAPed ZE41A alloy in a simulated body fluid, and then tailor the biodegradation rate of the UFG magnesium alloy containing rare-earth elements.

2. Experimental Section

A commercial as-cast ZE41A (Mg-4.9Zn-1.4RE-0.7Zr) alloy was used to prepare bulk UFG samples through a large number of ECAP passes. The multi-pass ECAP was conducted at 603 K using a rotary-die having a channel angle of 90° and through route A [8]. The dimension of the ECAP billet was 20 mm × 20 mm × 40 mm. These billets were continuously ECAP-fabricated from eight to 60 passes to obtain the uniformly distributed and UFG microstructure. Three kinds of ZE41A samples with various ECAP passes (eight, 16 and 60, respectively) were applied to investigate the effect of microstructure evolution on the bio-corrosion behavior. The microstructure was observed by means of Nikon Eclipse ME600 optical microscope(Nikon Instruments, Inc., Tokyo, Japan).

The degradation rate of the alloy during immersion can be monitored by the evolved hydrogen volume, and this method is easy to implement and is not prone to errors inherent in the weight loss method [19]. Herein, the ZE41A samples cut from the ECAP billets were immersed in 300 mL Dulbecco's modified eagle medium (DMEM) solution for 1–10 days at 310 K to study the hydrogen evolution rate variation with the immersion time. The DMEM solution was made using DMEM Cell Culture Media (without sodium bicarbonate, Merck Millipore Beijing Skywing technology Co., Ltd, Beijing, China), sodium bicarbonate (reagent grade) and distilled water. The initial pH value of the solution was 7.4, similar to that of human blood plasma.

Each sample was molded into epoxy resin with an exposed area for hydrogen evolution testing and electrochemical measurement, while the working surface was ground with SiC emery papers up to 2000 grit. The cylindrical test samples for eight and 16 ECAP passes had the diameter of 5 mm, while the exposed area of the plate samples for 60 ECAP passes was 7.6 mm × 1.8 mm. Hydrogen bubbles from each sample were collected into a burette, which detailed procedures have been reported elsewhere [20]. The hydrogen evolution rate of the 60-pass sample was also measured in 0.9 wt. % NaCl solution at room temperature as compared with the degradation performance in DMEM solution. Potentiodynamic polarization curves of the samples immersed for four days were measured in the simulated body fluid at 310 K, by means of an advanced electrochemical system of PARSTAT 2273 (Princeton Applied Research, Oak Ridge, TN, USA),. The three-electrode system has a saturated calomel electrode (SCE) as a reference and a platinum electrode as a counter and the sample as a working electrode. The polarization scan started from −2 V to −1 V at a scan rate of 1 mV/s.

After immersion testing for 2–10 days, the samples were removed from the DMEM solution, washed with distilled water and dried in air. The surfaces of the corroded samples were observed by HIROX KH-7700 Digital Microscope (Hirox Asia Ltd., Hong Kong, China), before and after the

corrosion products were removed. The corroded samples were cleaned with chromate acid (200 g/L CrO_3 + 10 g/L $AgNO_3$) for 5 min to remove corrosion products.

3. Results and Discussion

3.1. Microstructure of the ECAP-Fabricated ZE41A Alloy

Figure 1 presents optical micrographs of the as-cast ZE41A alloy with various ECAP passes. Primary microstructure of the as-cast alloy consists of equiaxed α-Mg grains and a small amount of net-like second phases, which are distributed mainly at α-Mg grain boundaries. After various ECAP passes, the microstructure of the alloy showed a continuous change with significant grain refinement of the Mg phase and homogeneous redistribution of broken second phases. Large elongated grains with a few percentages of ultrafine grains are observed for the eight-pass sample, and the second phases begin breaking and dispersing in the Mg matrix. Dynamic recrystallization (DRX) has been proven to be an efficient mechanism of grain refinement in the plastic deformation process [21]. After eight passes of ECAP, only small amounts of ultrafine grains are found due to incomplete recrystallization. The grains of the 16-pass sample are further refined with a more homogeneous dispersion of second phase particles. It shows that the percentage of ultrafine α-Mg grains increases with the ECAP passes. The alloy with a large pass number of ECAP can cause complete DRX to general equiaxed ultrafine grains. Hence, the 60-pass sample obtains UFG α-Mg grains (average size of about 2.5 μm) and fine second-phase particles which are homogeneously dispersed.

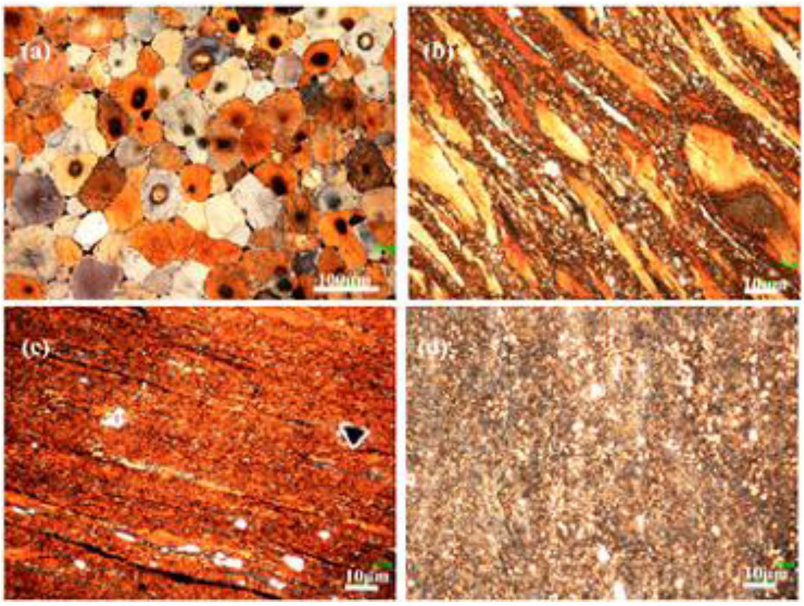

Figure 1. Micrographs of the ZE41A alloy before and after multi-pass ECAP: (**a**) As-cast; (**b**) eight passes; (**c**) 16 passes; (**d**) 60 passes.

Figure 2 presents the results of hydrogen evolution of the ECAPed samples immersed in DMEM solution and the 60-pass sample immersed in 0.9 wt. % NaCl solutions. The degradation process of the Mg alloy after multi-pass ECAP was time-dependent in the simulated body fluid. The hydrogen evolution of the samples immersed in DMEM solution went through three stages: an incubation period, a fast corrosion period and then a steady period. However, the 60-pass sample immersed in 0.9 wt. % NaCl solution basically shows a linear change. For those samples immersed in DMEM solution, a decrement of the incubation period with the increase of the ECAP pass was observed. It is probable due to the higher corrosive tendency of the Mg matrix acquiring lots of energy through the EACP processing. According to the method from Shi and Atrens [22], the corrosion rates of

the ECAPed samples in different immersion periods are summarized in Table 1. All three samples immersed in DMEM solution show a close corrosion rate which is less than 1.4 mm/y in the first period. The biggest corrosion rate is observed for the 60-pass sample in the fast corrosion period, which results in the earliest entrance into the steady period. During the steady period, the 60-pass sample shows the best corrosion resistance.

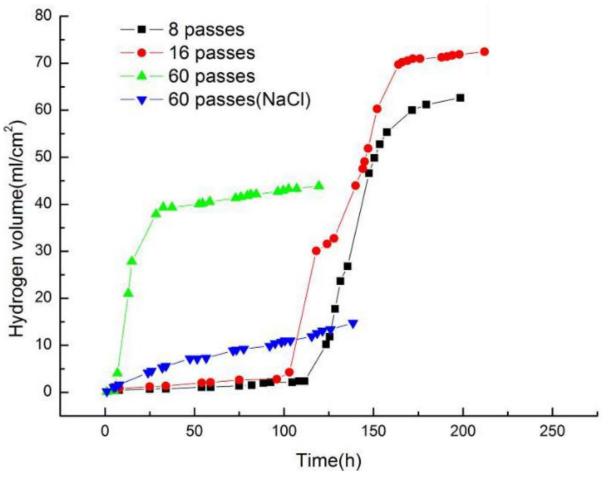

Figure 2. Hydrogen evolution diagrams of the ECAPed samples in DMEM solution.

Table 1. Corrosion rate of ECAPed samples in DMEM solution.

ECAP Pass	Duration of Incubation Period (h)	Hydrogen Evolution Rate (mL/cm²/h)			Corrosion Rate (mm/y)		
		Incubation Period	Fast Corrosion Period	Steady Period	Incubation Period	Fast Corrosion Period	Steady Period
8	120	0.019	1.38	0.075	1.04	75.48	4.10
16	96	0.022	1.45	0.050	1.20	79.30	2.73
60	5	0.025	2.60	0.045	1.37	142.20	2.46

Figure 3 presents potentiodynamic polarization curves of the ECAPed alloy after four days of immersion in DMEM solution. Three samples with different ECAP passes have similar polarization curves, indicating similar electrochemical corrosion behavior in the DMEM solution. Table 2 lists corresponding parameters including the corrosion potential (E_{corr}), the corrosion current density (I_{corr}) and the corrosion rate (CR_i) calculated from the polarization curves by Tafel extrapolation [22]. It shows that the increase of the ECAP pass makes the corrosion potential higher and the corrosion tendency lower. After immersion for four days, the corrosion current density of the 16-pass sample is the lowest but the 60-pass one is the biggest. Similar to the existing literature [22], the corrosion rates evaluated from polarization curves are lower than those evaluated from hydrogen evolution. Furthermore, the results of polarization measurement are consistent with the curves of hydrogen evolution in Figure 2. It is because the 16-pass sample after four days of immersion is at the incubation period but the 60-pass one is at the steady period. It seems that the anodic polarization plot of the 60-pass sample appears a passive zone.

Table 2. Parameters calculated from the potentiodynamic polarization curves in Figure 3.

ECAP Pass	8	16	60
E_{corr} (mV SCE)	−1358.59	−1352.57	−1337.43
I_{corr} (mA/cm^{-2})	1.71×10^{-2}	1.46×10^{-2}	2.08×10^{-2}
CR_i (mm/y)	0.39	0.33	0.47

Figure 4 presents surface morphologies of the corroded samples after different immersion times with/without corrosion products. It is obvious that pitting corrosion is the main corrosion type for the eight-pass sample and the 16-pass one, and the difference between the two samples is the amount and dimension of the corrosion pits. Several deep and obvious pits are observed for the eight-pass sample, while the surface of the 16-pass sample shows more but smaller pits. A reasonable argument can be deduced that the Mg matrix around second phases was corroded firstly, and the second-phase particles could not be held by the matrix and dropped from the site with the progress of the corrosion, thus leaving the pits after removing the corrosion products. Similar conditions and discussions can be found in other reports [17,18]. Therefore, the smaller pits were formed in the 16-pass sample with finer second-phase particles. It is notable that the 60-pass sample exhibits mainly a uniform corrosion. After 60 ECAP passes, the alloy achieved a large amount of ultrafine grains and homogeneously dispersed second-phase particles. It makes the pits in the 60-pass sample more uniform and smaller.

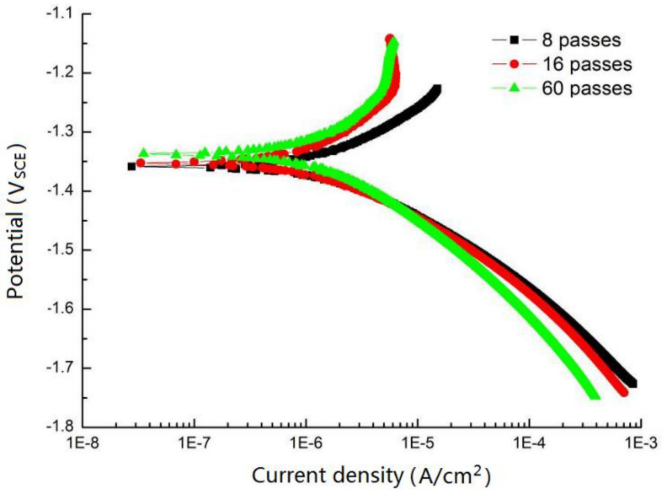

Figure 3. Potentiodynamic polarization curves of the ECAPed ZE41A alloy after immersion for four days in DMEM solution.

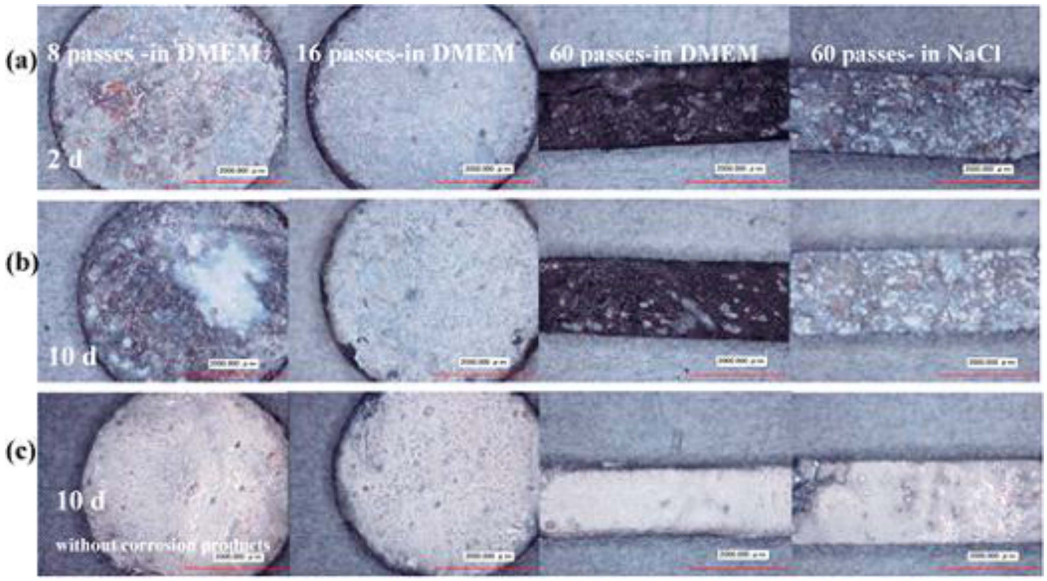

Figure 4. Morphology of the ECAPed samples after immersion for (**a**) two days; (**b**) 10 days; and (**c**) 10 days without corrosion products.

Considering that the degradation rate of Mg alloy in DMEM solution is one order of magnitude higher than that in Hank's solution [23], the corrosion rate of the 60-pass sample is significantly smaller than that of as-cast ZE41A Mg alloy reported by other research [15]. Hence, ECAP is an efficient method to improve the corrosion resistance of ZE41A Mg alloy in the physiological environment and tailor the lifetime of the biodegradable implant. This finding indicates that desirable retardation of the excessively rapid degradation of Mg alloys can be provided by grain ultrafining. It suggests that there is value in further investigating such effects by broadening both the alloy base and the processing techniques in order to control the appropriate biodegradation rate of Mg alloys for the clinical application.

4. Conclusions

The bio-corrosion behavior of a rare-earth magnesium alloy processed by multi-pass ECAP was investigated in a simulated body fluid. The present study shows that the biodegradation rate of the ZE41A alloy in the DMEM solution can be significantly reduced by grain ultrafining. The results open up a new possibility of tailoring the biodegradation of Mg alloys.

(1) The degradation process of the UFG Mg alloy was time-dependent in the simulated body fluid. The ZE41A alloy via different ECAP passes went through an incubation period, a fast corrosion period and then a steady period in DMEM solution. With the ECAP pass number increasing, the incubation period was shortened and the biodegradation rate at the steady corrosion period was decreased.

(2) The finer grains and more homogeneous second phases after more ECAP passes can improve the bio-corrosion resistance of the magnesium alloy. It results in a higher resistance toward localized corrosion and a lower biodegradation rate during the steady corrosion period. The UFG alloy for 60 ECAP passes has excellent corrosion resistance in DMEM solution.

(3) ECAP should be taken into consideration as an efficient technique to control the bio-corrosion rate of Mg alloys in the physiological environment and tailor the lifetime of the biodegradable implant, owing to its significant ability to acquire bulk UFG materials with homogeneous second phases.

Acknowledgments: This work is financially supported by Natural Science Foundation of Jiangsu Province of China (Grant No. BK20131373), Qing Lan Project and the Opening Project of Jiangsu Key Laboratory of Advanced Structural Materials and Application Technology (Grant No. ASMA201404).

Author Contributions: The work presented here was carried out in collaboration between all authors. Aibin Ma and Jinghua Jiang defined the research theme. Jinghua Jiang, Fan Zhang and Dan Song designed methods and experiments, carried out the laboratory experiments, analyzed the data, interpreted the results and wrote the paper. Jianqing Chen, Huan Liu and Mingshan Qiang co-designed experiments, discussed analyses and interpretation. All authors have contributed to, seen and approved the manuscript.

The author hopes that this paper can make its due contribution to the successful application of the high-performance Mg alloy implant.

Conflicts of Interest: The authors declare no conflict of interest.

References and Notes

1. Lee, J.Y.; Han, G.S.; Yu, C.K. Effects of impurities on the biodegradation behaviour of pure magnesium. *Met. Mater. Int.* **2009**, *15*, 955–961. [CrossRef]
2. Levesque, J.; Dube, D.; Fiset, M.; Mantovani, D. Materials and properties for coronary stents. *Adv. Mater. Process.* **2004**, *162*, 45–48.
3. Mani, G.; Feldman, M.D.; Patel, D.; Agrawal, C.M. Coronary stents: A materials perspective. *Biomaterials* **2007**, *28*, 1689–1710. [CrossRef] [PubMed]
4. Witte, F.; Hort, N.; Vogt, C.; Cohen, S.; Kainer, K.U.; Willumeit, R.; Feyerabend, F. Degradable biomaterials based on magnesium corrosion. *Curr. Opin. Solid State Mater. Sci.* **2008**, *12*, 63–72. [CrossRef]

5. Witte, F. The history of biodegradable magnesium implants: A review. *Acta Biomater.* **2010**, *6*, 1680–1692. [CrossRef] [PubMed]
6. Mueller, W.D.; Nascimento, M.L.; de Mele, M.F.L. Critical discussion of the results from different corrosion studies of Mg and Mg alloys for biomaterial applications. *Acta Biomater.* **2010**, *6*, 1749–1755. [CrossRef] [PubMed]
7. Staiger, M.P.; Pietak, A.M.; Huadmai, J.; Dias, G.J. Magnesium and its alloys as orthopedic biomaterials: A review. *Biomaterials* **2006**, *27*, 1728–1734. [CrossRef] [PubMed]
8. Valiev, R.Z.; Langdon, T.G. Principles of equal-channel angular pressing as a processing tool for grain refinement. *Prog. Mater.Sci.* **2006**, *51*, 881–981. [CrossRef]
9. Alvarez-Lopez, M.; Pereda, M.D.; del Valle, J.A.; Fernandez-Lorenzo, M.; Garcia-Alonso, M.C.; Ruano, O.A.; Escudero, M.L. Corrosion behaviour of AZ31 magnesium alloy with different grain sizes in simulated biological fluids. *Acta Biomater.* **2010**, *6*, 1763–1771. [CrossRef] [PubMed]
10. Sun, H.Q.; Shi, Y.N.; Zhang, M.X.; Lu, K. Plastic strain-induced grain refinement in the nanometer scale in a Mg alloy. *Acta Mater.* **2007**, *55*, 975–982. [CrossRef]
11. Figueiredo, R.B.; Langdon, T.G. Principles of grain refinement and superplastic flow in magnesium alloys processed by ECAP. *Mater. Sci. Eng.* **2009**, *501*, 105–114. [CrossRef]
12. Feng, X.M.; Ai, T.T. Microstructure evolution and mechanical behavior of AZ31 Mg alloy processed by equal-channel angular pressing. *Trans. Nonferrous Metals Soc. China* **2009**, *19*, 293–298. [CrossRef]
13. Ding, R.; Chung, C.; Chiu, Y. Effect of ECAP on microstructure and mechanical properties of ZE41 magnesium alloy. *Mater. Sci. Eng.* **2010**, *527*, 3777–3784. [CrossRef]
14. Huang, P.; Li, J.; Zhang, S.; Chen, C.; Han, Y.; Liu, N.; Xiao, Y.; Wang, H.; Zhang, M.; Yu, Q.; *et al*. Effects of lanthanum, cerium, and neodymium on the nuclei and mitochondria of hepatocytes: Accumulation and oxidative damage. *Environ. Toxicol. Pharmacol.* **2011**, *31*, 25–32. [CrossRef] [PubMed]
15. Song, G. Control of biodegradation of biocompatable magnesium alloys. *Corros. Sci.* **2007**, *49*, 1696–1701. [CrossRef]
16. Feyerabend, F.; Fischer, J.; Holtz, J.; Witte, F.; Willumeit, R.; Drucker, H.; Vogt, C.; Hort, N. Evaluation of short-term effects of rare earth and other elements used in magnesium alloys on primary cells and cell lines. *Acta Biomater.* **2010**, *6*, 1834–1842. [CrossRef] [PubMed]
17. Zhang, E.; Yang, L. Microstructure, mechanical properties and bio-corrosion properties of Mg-Zn-Mn-Ca alloy for biomedical application. *Mater. Sci. Eng.* **2008**, *497*, 111–118. [CrossRef]
18. Gao, J.H.; Guan, S.K.; Ren, Z.W.; Zhu, S.J.; Wang, B. Homogeneous corrosion of high pressure torsion treated Mg-Zn-Ca alloy in simulated body fluid. *Mater. Lett.* **2011**, *65*, 691–693. [CrossRef]
19. Song, G.; Atrens, A. Understanding magnesium corrosion-a framework for improved alloy performance. *Adv. Eng. Mater.* **2003**, *5*, 837–858. [CrossRef]
20. Abidin, N.I.Z.; Martin, D.; Atrens, A. Corrosion of high purity Mg, AZ91, ZE41 and Mg2Zn0.2Mn in Hank's solution at room temperature. *Corros. Sci.* **2011**, *53*, 862–872. [CrossRef]
21. Galiyev, A.; Kaibyshev, R.; Gottstein, G. Correlation of plastic deformation and dynamic recrystallization in magnesium alloy ZK60. *Acta Materi.* **2001**, *49*, 1199–1207. [CrossRef]
22. Shi, Z.; Liu, M.; Atrens, A. Measurement of the corrosion rate of magnesium alloys using Tafel extrapolation. *Corros. Sci.* **2010**, *52*, 579–588. [CrossRef]
23. Xin, Y.; Hu, T.; Chu, P.K. Influence of test solutions on in vitro studies of biomedical magnesium alloys. *J. Electrochem. Soc.* **2010**, *157*, C238–C243. [CrossRef]